Thermal Analysis and Optical Microscopy of Modified Polystyrene/Poly(ethyl acrylate) Blends Containing Specific Interactions

Elliot P. Douglas, Kazuo Sakurai,† and William J. MacKnight*

Department of Polymer Science and Engineering, University of Massachusetts, Amherst, Massachusetts 01003

Received June 5, 1991; Revised Manuscript Received July 30, 1991

ABSTRACT: The effect of specific interactions on the mixing behavior of sulfonated polystyrene (SPS) and ethyl acrylate/4-vinylpyridine copolymers (EAVP) has been examined using differential scanning calorimetry (DSC), dynamic mechanical thermal analysis (DMTA), and optical microscopy. For both the acid and zinc-neutralized forms of SPS, blends at a 2% substitution level show two phases consisting of the pure components, although DSC data indicate that some enhanced mixing compared to the unfunctionalized blend has occurred at the interface. Blends of higher substitution levels show predominantly a mixed phase by DMTA. Optical microscopy shows that 2% interacting groups is enough to result in a dramatic change in the blend morphology; the domains become much smaller and more uniform in size compared to the unfunctionalized blend. The results are interpreted in terms of a model in which the interactions are considered to be cross-links, and thus phase separation occurs for all blends to the extent allowed by the topological constraints imposed by the interacting groups.

Introduction

It is well-known that polymer blends are generally not miscible. This is due to the very low entropy of mixing of long polymer chains and the unfavorable enthalpy of mixing of most polymer pairs due to van der Waals interactions. There are, however, an increasing number of polymer pairs that do exhibit miscibility. One classic example is the blend of polystyrene and poly(vinyl methyl ether), which exhibits miscibility over the entire composition range.[1] Miscible homopolymer blends generally require some type of specific interaction between the two components to provide a negative enthalpy of mixing. In the case of polystyrene and PVME, it is believed that such an interaction occurs between the ether oxygen and the phenyl ring.[2]

Over the years there have been many studies of ways to increase the compatibility of otherwise immiscible polymers. The methods used have included physically co-cross-linking the two components,[3] the introduction of physical entanglements through the formation of interpenetrating networks,[4] hydrogen-bonding interactions,[5] and donor/acceptor complexes.[6] All of these approaches result in some enhancement of mixing.

Of particular interest is the work carried out by Eisenberg and co-workers. In a series of experiments they investigated the mixing behavior of otherwise immiscible polymers that are modified to contain acid/base, ion/ion, and ion/dipole interactions.[7-11] In general, their experiments show that polymers containing a sulfonic acid group mixed with polymers containing vinylpyridine exhibit a single loss peak in dynamic mechanical experiments above a substitution level of 5%, even when the parent polymers are completely immiscible. This result holds for a wide variety of polymer pairs, including polystyrene and poly(ethyl acrylate),[7,8] polystyrene and polyisoprene,[8] and polyphenylene and poly(ethyl acrylate).[9] Similar studies have been done by other groups on systems in which the acid group has been neutralized with a transition-metal ion.[12,13] These systems also show enhanced miscibility, due to a coordination interaction between the metal ion and pyridine.

We have decided to extend the previous work in this area by systematically examining the effect of substitution level and type of interaction. To date, no one has directly compared the acid/base interaction with the coordination interaction. There have also been no systematic studies of the morphology of these systems. This first report describes the thermal behavior and some results on morphology for the blends of sulfonated polystyrene in both the acid and zinc-neutralized forms with copolymers of ethyl acrylate and 4-vinylpyridine. This system has been chosen since it is the most studied to date, and thus our work serves to build on previous results.

Experimental Section

Polymer Synthesis. The sulfonated polystyrenes in both the acid (HSPS) and zinc-neutralized (ZSPS) forms were kindly provided by Exxon Research and Engineering Co. Sulfonation levels and molecular weights are given in Table I. The copolymers of ethyl acrylate and 4-vinylpyridine (EAVP) were prepared by free-radical polymerization in solution. The reactivity ratios for this polymerization are $r_{EA} = 0.29$ and $r_{VP} = 2.58$.[14] A typical polymerization consisted of reacting 300 g of monomer and 7 g of AIBN in 700 mL of methanol at 60 °C for times varying from 20 to 90 min, depending on the pyridine content. Conversions for the polymerizations were approximately 20–30%. The polymers were purified by precipitating into water and drying for 3 days at 60 °C under vacuum. Pyridine contents determined by elemental analysis and molecular weights determined by GPC based on polystyrene standards are given in Table I.

Blending. All blends were prepared to have equal numbers of sulfonate and pyridine groups. The acid blends were prepared according to the procedure of Smith and Eisenberg.[7] The HSPS and EAVP were dissolved separately in THF at a concentration of 1% (w/v). The EAVP solution was added to the HSPS solution dropwise over a period of about 45 min while stirring, and stirring was continued an additional 30 min after addition ended. In all cases a gel was formed, and this gel was removed from the solvent. The zinc blends were prepared in the same fashion, except that DMF was used as the solvent due to limited solubility of the zinc ionomers in THF, and the blends were isolated by precipitating into distilled water. All blends were dried at 60 °C for 3 days under vacuum. The nomenclature of the blends is as follows: the first number indicates the sulfonation level of the SPS in mole percent, the letter indicates the counterion, and the second

† Permanent address: Research and Development Center, Kanebo Ltd., 1-5-90 Tomobuchi-cho, Miyakojima-ku, Osaka, Japan.

0024-9297/91/2224-6776$02.50/0

Table I
Characteristics of Blend Precursors

polymer	ionic content, mol %	M_n	M_w
0SPS	0	100 000	250 000
2HSPS	1.71	100 000	250 000
5HSPS	5.7	100 000	250 000
8HSPS	7.6	100 000	250 000
2ZSPS	2.1	100 000	250 000
5ZSPS	5.5	100 000	250 000
7ZSPS	7.25	100 000	250 000
0EAVP	0	230 000	890 000
2EAVP	2.4	230 000	730 000
5EAVP	5.2	201 000	406 000
10EAVP	10.6	161 000	315 000

Table II
Characteristics of Blends

blend desig	counterion in SPS	sulfonation level in SPS, mol %	VP content in EAVP, mol %	wt fraction of EAVP in blend
00		0	0	0.50
2H2	H^+	1.71	2.4	0.40
5H5	H^+	5.7	5.2	0.50
8H10	H^+	7.6	10.6	0.40
2Z2	Zn^{2+}	2.1	2.4	0.45
5Z5	Zn^{2+}	5.5	5.2	0.51
7Z10	Zn^{2+}	7.25	10.6	0.37

number indicates the pyridine content of the ethyl acrylate/4-vinylpyridine copolymer in mole percent. Characteristics of the blends are given in Table II.

Differential Scanning Calorimetry (DSC). DSC analysis was done on a Du Pont Instruments DSC 10. Calibration was done with indium and mercury standards. The sample size for all DSC runs was approximately 10 mg. The precursor polymers were first heated to 150 °C for 1 min to obtain good contact between the sample and the pan, then quenched with liquid nitrogen, and scanned from 30 to 150 °C at 20 °C/min for the SPS's and from −120 to +25 °C at 20 °C/min for the EAVP's. The blends were placed in the DSC pan as blended, heated to 150 °C for 2 min to obtain good contact between the sample and the pan, quenched with liquid nitrogen, and scanned from −120 to +150 °C at 20 °C/min. Determination of glass transition temperatures, changes in heat capacity, and transition widths were determined manually. The glass transition is given as the temperature at which half the change in heat capacity occurs; the transition width is the total temperature range over which the heat capacity change occurs. All samples were run at least twice to check reproducibility.

Dynamic Mechanical Thermal Analysis (DMTA). DMTA was done on a Polymer Laboratories DMTA in the single cantilever bending mode. Samples were prepared by compression molding at 175 °C under vacuum for 6 min. All samples were run at 2 °C/min at five frequencies (0.33, 1, 3, 10, and 30 Hz) using a constant 64-μm peak-to-peak displacement and an active sample size of 2 mm × 10 mm × 0.5 mm. The EAVP's were run from −100 to +20 °C, the SPS's from 30 to 140 °C, and the blends from −100 to +130 °C. All of the blends and some of the precursors were run twice each to check reproducibility. Transition temperatures are given as the peak in tan δ at 1 Hz. Transition widths are given as the half-width at half-height (HWHH) of the tan δ peak at 1 Hz.

Optical Microscopy. Samples for optical microscopy were prepared by compression molding the blends at 175 °C for 6 min into films a few microns thick. Images were obtained using Hoffman modulation contrast.

Results and Discussion

Thermal analysis data from both DSC and DMTA for all the precursor polymers are given in Table III. As expected, the glass transition temperatures increase with increasing substitution level for each type of polymer. It should also be noted that the widths of the transitions are very narrow.

Figure 1 shows the DSC curves for all of the blends, and the data are summarized in Table IV. The unfunctionalized and 2% functionalized blends clearly show two T_g's. To determine the presence of any enhanced compatibility for these blends, the weight fraction of interface material was calculated using the equation of Beckman et al.[15] The calculations for blends 00, 2H2, and 2Z2 indicate that the weight fraction of material in the interface is 0.05, 0.15, and 0.31, respectively. These values are not absolute and are subject to somewhat large errors, but they indicate that even for two-phase blends the presence of a small number of interacting groups provides some enhanced mixing.

For blends of higher substitution level the choice of transitions as given in Table IV is somewhat arbitrary. Nevertheless, it is clear that a rather dramatic change has occurred with these materials. The presence of the very broad transitions in the DSC traces implies that the blends

Table III
DSC and DMTA Data for Blend Precursors

polymer	DSC T_g, °C	DSC ΔC_p, J/(g °C)	DSC ΔT_g, °C	DMTA T_g,[a] °C	DMTA ΔT_g,[b] °C
0SPS	97.5 ● 3.0	0.30 ± 0.05	8.3 ± 3.0	105.0 ± 1.0	4.3 ± 1.0
2HSPS	103.3	0.31	8.6	110.3	5.3
5HSPS	110.2	0.34	11.7	117.0	5.5
8HSPS	111.1	0.33	10.9	119.5	7.3
2ZSPS	108.2	0.28	10.6	118.5	4.5
5ZSPS	115.5	0.30	15.4	121.0	8.0
7ZSPS	120.5	0.32	19.1	128.5	9.5
0EAVP	−15.9	0.44	7.5	−8.5	6.5
2EAVP	−13.9	0.49	8.1	−4.0	7.5
5EAVP	−10.0	0.42	8.3	−2.0	3.5
10EAVP	−7.3	0.48	8.6	2.0	4.5

[a] Taken as the peak in tan δ at 1 Hz. [b] Taken as the half-width at half-height of the peak in tan δ at 1 Hz.

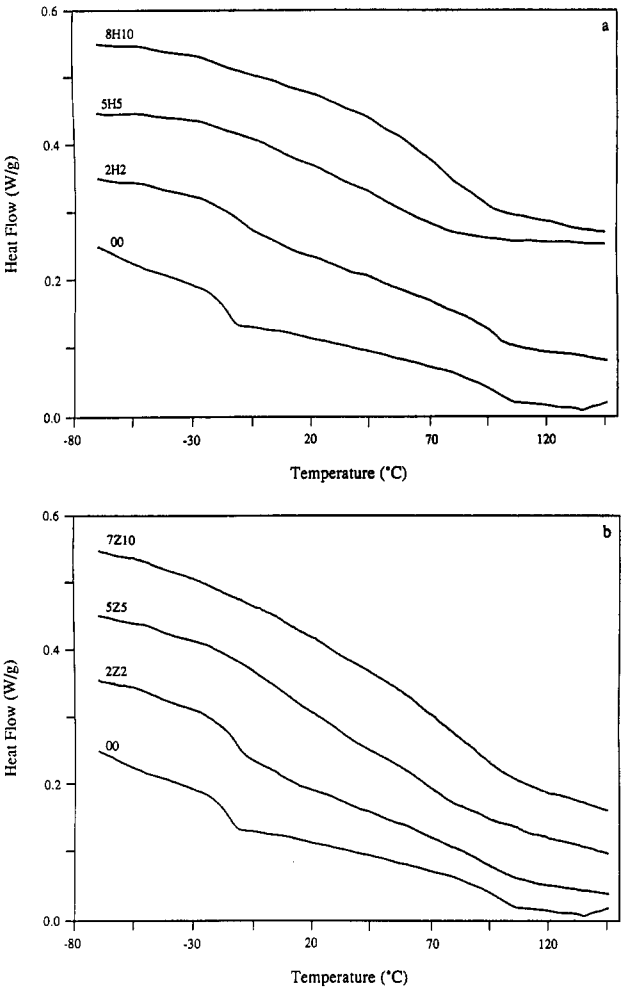

Figure 1. DSC curves for (a) acid blends and (b) zinc blends.

Table IV
DSC Data for Blends

blend	T_g, °C	ΔC_p, J/(g °C)	ΔT_g, °C
00	−16.4 ± 5.0	0.17 ● 0.1	8.0 ● 5.0
	94.5	0.17	17.6
2H2	−11.5	0.15	15.9
	96.5	0.17	21.5
5H5	37.9	0.52	97.0
8H10	72.9	0.51	47.7
2Z2	−13.2	0.17	10.7
	91.3	0.10	10.6
5Z5	0.4	0.23	29.6
	66.9	0.13	20.7
7Z10	82.0	0.37	41.1

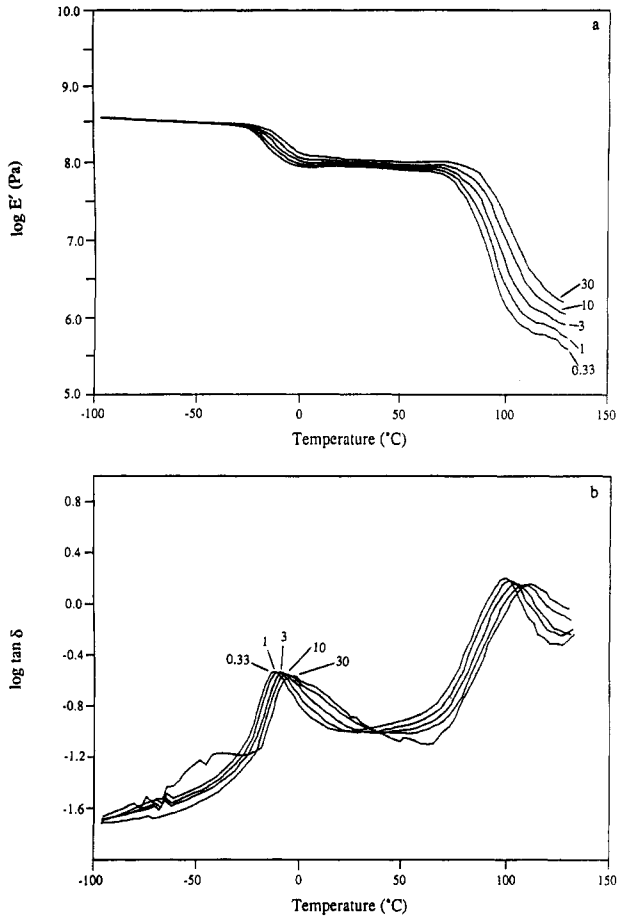

Figure 2. Multifrequency DMTA curves of (a) storage modulus and (b) tan δ for blend 00. The numbers in the figure indicate the frequency in hertz.

are still phase separated, but on a scale smaller than can be detected by DSC.

As a more sensitive probe of phase behavior, the blends were analyzed using dynamic mechanical measurements. Figures 2 and 3 show typical multifrequency runs for blends 00 and 8H10. Figures 4 and 5 show the results for all the blends at 1 Hz. Results for all the blends are summarized in Table V.

The storage modulus curves show that blends with 2% interacting groups are phase separated, as evidenced by the two-step decrease in the modulus. For blends with 5% or greater interacting groups, the modulus curves show only a single, although broad, decrease. However, careful examination of the loss curves clearly indicates that even these blends exhibit some phase separation. These blends appear to consist of a single major phase and a very small amount of a second phase. Further, the breadths of the transitions indicate that there is a substantial range of compositions even within a single phase. The presence of

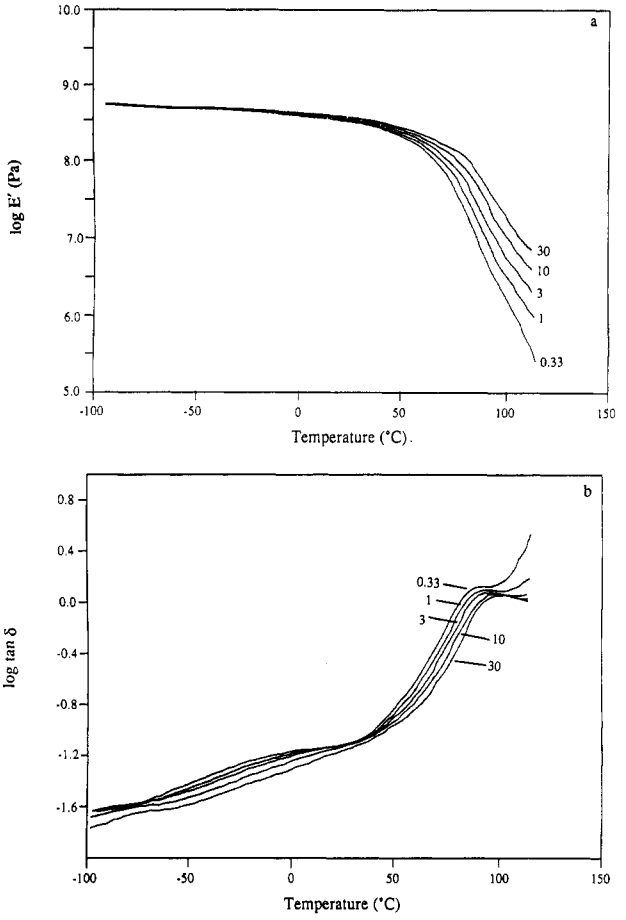

Figure 3. Multifrequency DMTA curves of (a) storage modulus and (b) tan δ for blend 8H10. The numbers in the figure indicate the frequency in hertz.

a single main peak seems to show that the predominant phase in these blends is a miscible phase.

Phase compositions for the phases in each blend were calculated from the experimental T_g's based on the Fox equation:

$$\frac{1}{T_g} = \frac{W_1}{T_{g_1}} + \frac{W_2}{T_{g_2}}$$

where T_g is the glass transition temperature of the phase, T_{g_1} and T_{g_2} are the glass transition temperatures of the pure components, and W_1 and W_2 are the weight fractions of the pure components in the phase.

The results of the calculations are shown in Figure 6 and listed in Table V. For blends at 2% substitution level the phases are essentially pure. For 5% substitution level the upper composition decreases dramatically, indicating the presence of much greater mixing. As stated before, this upper composition represents a miscible phase. Comparison with Table II might seem to contradict this statement, since the calculated compositions do not match the overall bulk compositions given in Table II. However, the Fox equation is not expected to be accurate for this system, since it does not take into account the effect of specific interactions. In fact, the Fox equation predicts a T_g for a miscible system that is lower than simple linear additivity would give, while specific interactions would be expected to raise T_g above the value from linear additivity. Work is currently in progress to attempt to quantify the effect that the specific interactions have on T_g.

To image the morphology of the blends directly, Hoffman modulation contrast optical microscopy was used. Typical micrographs are shown in Figure 7. Blend 00

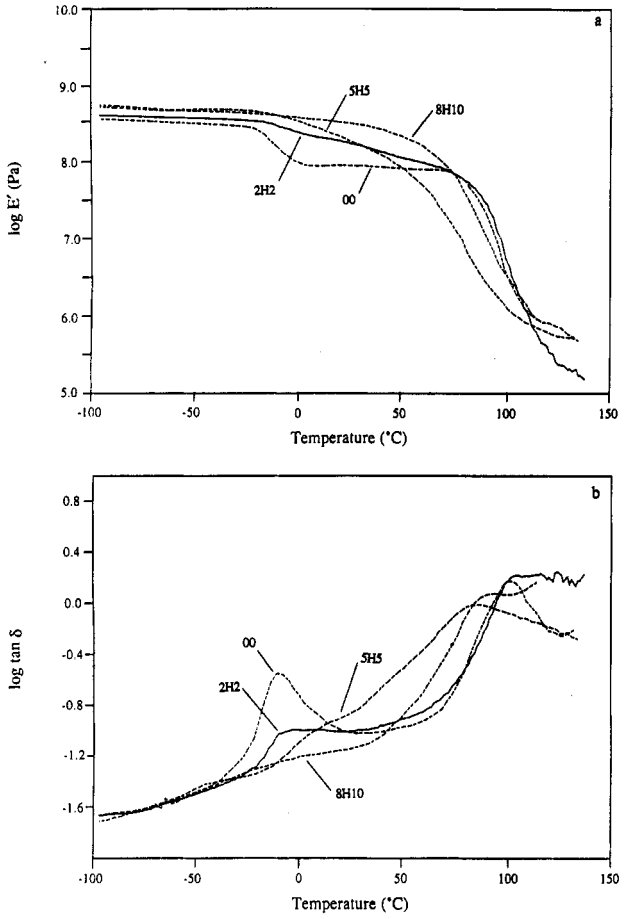

Figure 4. DMTA curves of (a) storage modulus and (b) tan δ for all acids blends at 1 Hz.

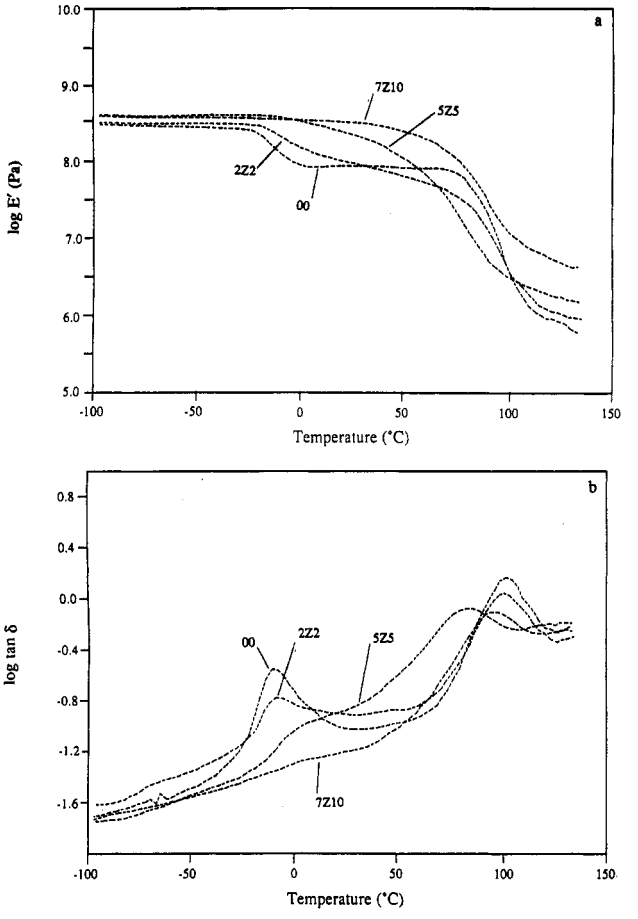

Figure 5. DMTA curves of (a) storage modulus and (b) tan δ for all zinc blends at 1 Hz.

Table V
DMTA Data for Blends

blend	T_g,[a] °C	ΔT_g,[b] °C	phase comp (wt fraction of EAVP)[c]
00	-9.0 ● 3.0	8.3 ● 3.0	1.00 ● 0.05
	102.8	11.8	0.01
2H2	-6.0	12.0	1.03
	105.5	12.3	0.03
5H5	24.5	25.3	0.71
	90.5	25.0	0.17
8H10	10.0	54.5	0.91
	92.8	15.8	0.17
2Z2	-8.0	11.3	1.05
	100.5	13.0	0.11
5Z5	14.8	26.5	0.81
	83.8	19.5	0.23
7Z10	9.0	38.0	0.92
	96.0	16.0	0.19

[a] Taken as the peak in tan δ at 1 Hz. [b] Taken as the half-width at half-height of the peak in tan δ at 1 Hz. [c] Calculated from the Fox equation.

shows a typical phase-separated structure with domain sizes ranging from 5 to 30 μm. The addition of only 2% interacting groups clearly has a dramatic effect on the morphology; the domains become much smaller and much more regular in size and distribution, with sizes on the order of 2–5 μm. The reasons for this change will be discussed further below. Blend 5H5 shows no evidence of phase separation; the features seen are surface features which aid in focusing. All other blends look identical to 5H5.

In formulating a model to explain the mixing behavior of these systems, one must consider that the sequences of polystyrene and poly(ethyl acrylate) between the inter-

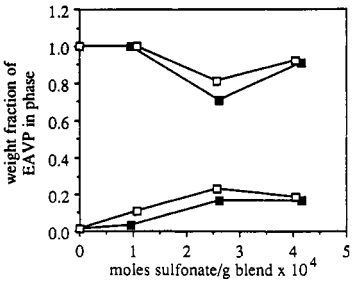

Figure 6. Phase compositions for all blends from the DMTA data for (■) acid blends and (□) zinc blends. Calculations were done using the Fox equation.

acting groups remain immiscible despite the presence of specific interactions. Thus, phase separation will occur to the extent allowed by the topological constraints imposed by the interactions. A schematic diagram of this model is shown in Figure 8. It is evident from this model that the detection of a one-phase or a two-phase system depends on two factors. First, the number of interacting groups will determine the size of the phases. Second, the resolution of the experiment will determine how many phases are detected. Experiments that observe length scales longer than the distance between interacting groups will detect only a single phase, while experiments that observe length scales shorter than that distance will detect two phases. This model is not a new one. It has been stated in various forms in previous studies[3-5] and is the direct conclusion of a theoretical treatment by Brereton and Vilgis.[16]

The experimental results can now be interpreted in light of this model. Phase separation is seen more clearly by DMTA than DSC at higher substitution levels because it

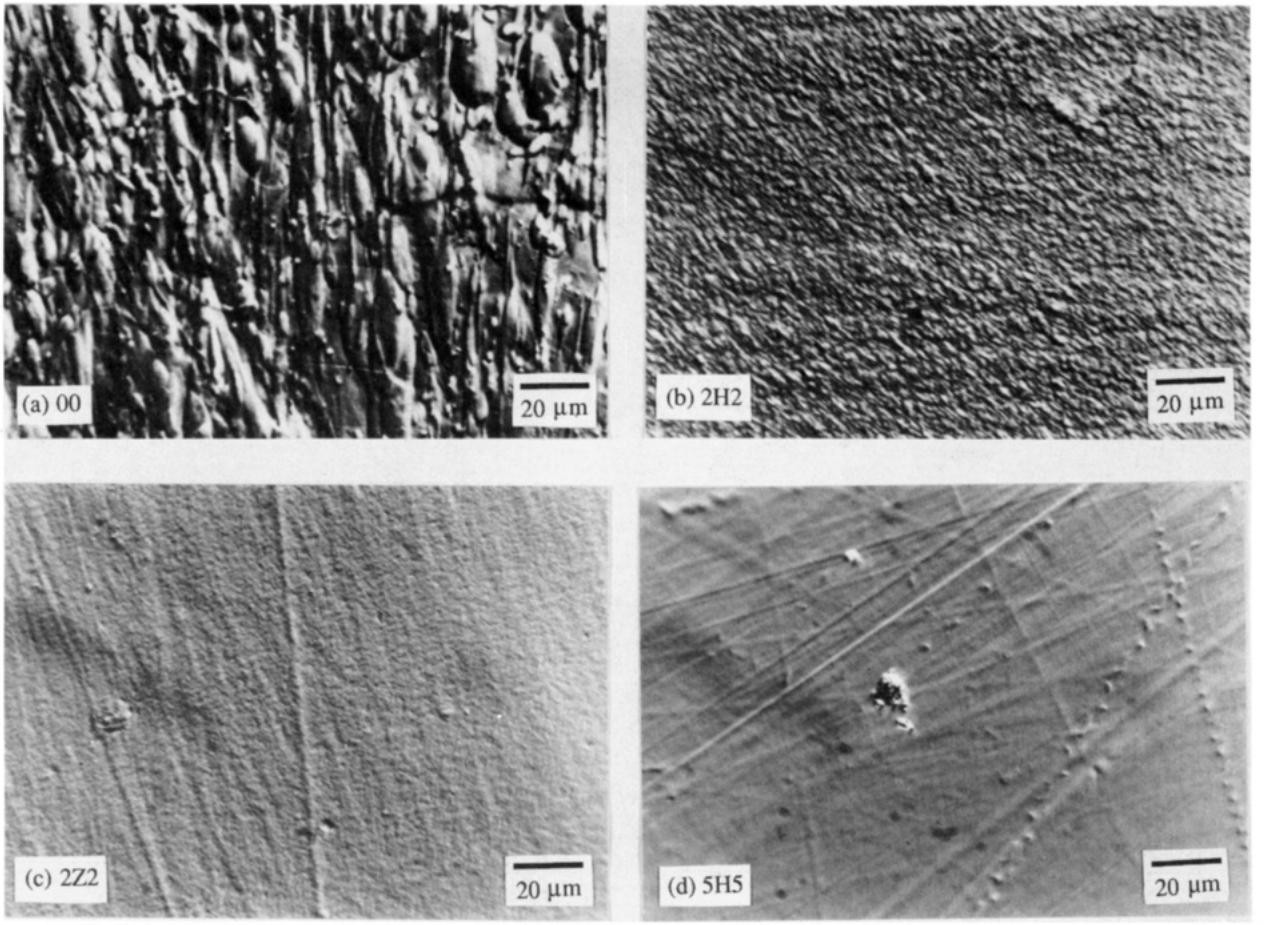

Figure 7. Typical optical micrographs for blends (a) 00, (b) 2H2, (c) 2Z2, and (d) 5H5. The blends not shown are identical to blend 5H5.

Figure 8. Schematic diagram of a model of mixing in the blends. The thin solid line represents polystyrene, the dotted line represents poly(ethyl acrylate), and the thick solid lines represent the interactions between sulfonate and pyridine groups.

has a higher spatial resolution. Even by DMTA, however, the main transition seen is due to a mixed phase. In terms of the model, most of the domain sizes are smaller than can be detected by DMTA, and a single phase is detected. The presence of a low-temperature phase is likely due to a distribution of distances between interacting groups, resulting in a few domains large enough to be detected by DMTA. This is especially likely considering that the conversions used in synthesizing the EAVP's (20–30%) are likely to introduce some drift in the copolymerization, and the reactivity ratios are such that drift would lead to longer ethyl acrylate sequences.

The changes in morphology for 2H2 and 2Z2 compared to the unfunctionalized blend are also explained by this model. The domain sizes are determined by the presence of the interacting groups, and since the interacting groups are distributed somewhat uniformly along the chain, it is expected that the domains would become more uniform in size. It should be noted that for a 2% functional level the chain contour length between interacting groups is approximately 200 Å, while the optical micrographs indicate domain sizes at least 10 times that. Clearly, not all the functional groups are interacting with each other, and recent infrared spectroscopy data confirm this observation.[17]

Conclusions

The experimental results show that phase separation takes place for all blends, regardless of substitution level. However, the nature of the phase separation changes. For blends with 2% interacting groups, the phases consist of the pure components. Calculations of the interface fraction from DSC data show that even these blends exhibit some enhanced mixing. For blends with 5% or more interacting groups, DMTA detects a predominant mixed phase and a minor EAVP-rich phase. In terms of the model, this result indicates a distribution of distances between interacting groups. The mixed phase results from sequence lengths smaller than the resolution of DMTA. Only a few sequences are long enough to result in domains large enough to be detected by DMTA. The change in morphology observed at a 2% substitution level is also a result of the constraints of the interactions.

The experimental results also show that there is no difference between the acid/base interaction and the coordination interaction. It is not the type or strength of the interaction that is important in determining the mixing behavior of these systems, but simply the presence of the interactions which can be considered as cross-links. Lu and Weiss have used a modified Flory–Huggins equation to describe mixing in similar systems.[18,19] In this approach the favorable interactions are considered to lead to an

overall negative free energy of mixing. However, previous studies on co-cross-linked systems and interpenetrating networks have also shown enhanced compatibility.[3,4] These systems do not contain any favorable interactions and thus support the concept that the interacting groups, although ionic, act as cross-links.

It should be pointed out that Eisenberg has presented a ranking of interacting group strength based on the levels of miscibility enhancement observed for different types of interactions in the polystyrene/poly(ethyl acrylate) system.[11] In terms of our model, this ranking is due to differences in the number of interactions that take place. The differences result from an equilibrium between the formation of the interactions and the repulsion of unlike polymer pairs during blending, and this equilibrium is a function of interaction strength. Given equal numbers of interactions, the level of mixing will be the same regardless of the type of interaction.

It should also be noted that Natansohn and Eisenberg have concluded from NMR experiments that similar blends in DMSO solution are intimately mixed.[20] This result may be due to the presence of the solvent. In ionizing solvents such as DMSO it is likely that the ionic chains adopt an extended-chain conformation due to the well-known polyelectrolyte effect.[21] In this case, as the ionic groups form the interaction the two different chains will also be brought together along their entire length, even though they phase separate in the bulk.

One consequence of this model is that all of the blends should be completely phase separated into pure components at very small length scales. Experiments are currently underway to test this hypothesis using electron microscopy and NMR relaxation time measurements.

Acknowledgment. We thank Dr. Dennis G. Peiffer and Dr. Robert D. Lundberg of Exxon Research and Engineering Co. for providing the sulfonated polystyrenes, GPC analysis, and many helpful discussions. K.S. thanks Kanebo Ltd. for providing him the opportunity to work on this project. Funding was kindly provided by U.S. Army Grant DAAL03-91-G-0127.

References and Notes

(1) Kwei, T. K.; Nishi, T.; Roberts, R. F. *Macromolecules* **1974**, *7*, 667.
(2) Walsh, D. J.; Rostani, S. *Adv. Polym. Sci.* **1985**, *70*, 119.
(3) Yoshimura, N.; Fujimoto, K. *Rubber Chem. Technol.* **1969**, *42*, 1009.
(4) Sperling, L. H.; Taylor, D. W.; Kirkpatrick, M. L.; George, H. F.; Bardman, D. R. *J. Appl. Polym. Sci.* **1970**, *14*, 73.
(5) Pearce, E. M.; Kwei, T. K.; Min, B. Y. *J. Macromol. Sci., Chem.* **1984**, *A21*, 1181.
(6) Ohno, N.; Kumanotani, J. *Polym. J.* **1979**, *11*, 947.
(7) Smith, P.; Eisenberg, A. *J. Polym. Sci., Polym. Lett. Ed.* **1983**, *21*, 223.
(8) Eisenberg, A.; Smith, P.; Zhou, Z.-L. *Polym. Eng. Sci.* **1982**, *22*, 1117.
(9) Murali, R.; Eisenberg, A. *Poly. Prepr. (Am. Chem. Soc., Div. Polym. Sci.)* **1986**, *27* (1), 343.
(10) Zhang, X.; Eisenberg, A. *Polym. Adv. Technol.* **1990**, *1*, 9.
(11) Zhang, X.; Eisenberg, A. *J. Polym. Sci., Part B: Polym. Phys.* **1990**, *28*, 1841.
(12) Agarwal, P. K.; Duvdevani, I.; Peiffer, D. G.; Lundberg, R. D. *J. Polym. Sci., Part B: Polym. Phys.* **1987**, *25*, 839.
(13) Register, R. A.; Sen, A.; Weiss, R. A.; Li, C.; Cooper, S. *J. Polym. Sci., Part B: Polym. Phys.* **1989**, *27*, 1911.
(14) Niwa, M.; Matsumoto, T.; Kagami, M.; Kajiyama, K. *Sci. Eng. Rev., Doshisha Univ.* **1984**, *25*, 192.
(15) Beckman, E. J.; Karasz, F. E.; Porter, R. S.; MacKnight, W. J.; Van Hunsel, J.; Koningsveld, R. *Macromolecules* **1988**, *21*, 1193.
(16) Brereton, M. G.; Vilgis, T. A. *Macromolecules* **1990**, *23*, 2044.
(17) Sakurai, K.; Douglas, E. P.; MacKnight, W. J. *Macromolecules*, to be submitted.
(18) Lu, X.; Weiss, R. A. *Polym. Mater. Sci. Eng.* **1991**, *64*, 75.
(19) Lu, X.; Weiss, R. A. *Polym. Mater. Sci. Eng.* **1991**, *64*, 163.
(20) Natansohn, A.; Eisenberg, A. *Macromolecules* **1987**, *20*, 323.
(21) Fitzgerald, J. J.; Weiss, R. A. *J. Macromol. Sci., Rev. Macromol. Chem. Phys.* **1988**, *C28*, 99.

Registry No. EAVP (copolymer), 28963-65-7.